Short communication

Gasoline-fueled solid oxide fuel cell with high power density

Xiaoxue Hou [a], Oscar Marin-Flores [b], Byeong Wan Kwon [a], Jinsoo Kim [c], M. Grant Norton [b, **], Su Ha [a, c, *]

[a] Voiland School of Chemical Engineering and Bioengineering, Washington State University, P.O. Box 642710, Pullman, WA 99164-2710, USA
[b] School of Mechanical and Materials Engineering, Washington State University, P.O. Box 642920, Pullman, WA 99164-2920, USA
[c] Department of Chemical Engineering, Kyung Hee University, Yongin, Kyunggi-do 449-701, Republic of Korea

HIGHLIGHTS

- MoO_2-based anode was fabricated via an electrospray process for SOFC applications.
- MoO_2-based SOFC successfully operated under direct gasoline-fed operating condition.
- MoO_2-based SOFC produced a high initial power density >3 W cm^{-2} at 750 °C.
- MoO_2-based SOFC maintained a power density output of ~2 W cm^{-2} at 0.6 V over 24 h.

GRAPHICAL ABSTRACT
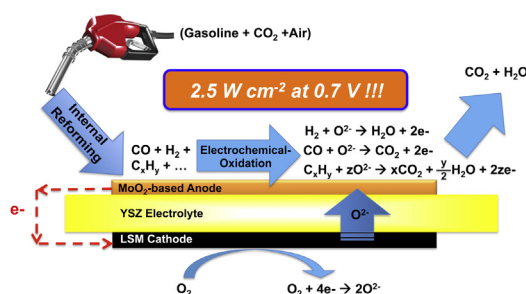
ARTICLE INFO

ABSTRACT

This short communication describes the performance of a solid oxide fuel cell (SOFC) fueled by directly feeding premium gasoline to the anode without using external reforming. The novel component of the fuel cell that enables such operation is the mixed conductivity MoO_2-based anode. Using this anode, a fuel cell demonstrating a power density >3.0 W cm^{-2} at 0.6 V was successfully fabricated. Over a 24 h period of operation, the open cell voltage remained stable at ~0.9 V. At the cell voltage of 0.6 V, its current density dropped over the first 7 h to a value of ~3.0 A cm^{-2}, where it stayed for the remaining 17 h of the test with a minor fluctuation. Power density of ~2.0 W cm^{-2} at 0.6 V was still measured after 24 h on stream with a continuous feed of gasoline. Scanning electron microscopy (SEM) examination of the anode surface pre- and post-testing showed no evidence of coking, which hints at the reason for the observed stability under the harsh cell operating conditions. The implication of this preliminary study is that an SOFC using a MoO_2-based anode has potential for generating electrical power from gasoline for future hybrid electric vehicles.

© 2014 Elsevier B.V. All rights reserved.

1. Introduction

Solid oxide fuel cells (SOFCs) have been widely studied as an attractive energy conversion device due to their low emission and high conversion efficiency [1–6]. One of the important advantages of SOFCs over other types of fuel cell, such as low temperature polymer electrolyte membrane (PEM) fuel cells, is that they are able to utilize various types of fuels including most liquid hydrocarbons, simple alcohols, and biomass-derived oxygenated hydrocarbons [7–9]. This advantage eliminates the need for specific or highly purified hydrogen fuels and allows the use of the existing fuel distribution infrastructure. Because of simplified fuel processing requirements and their ability to operate with complex hydrocarbon fuels, SOFCs have been proposed for on-board electrical power

* Corresponding author. Voiland School of Chemical Engineering and Bioengineering, Washington State University, P.O. Box 642710, Pullman, WA 99164-2710, USA. Tel.: +1 509 335 3786; fax: +1 509 335 4806.
** Corresponding author.
E-mail addresses: mg_norton@wsu.edu (M.G. Norton), suha@wsu.edu (S. Ha).

generation of commercial aircraft such as the Boeing 777 [10]. Analysis by Boeing projected a 75% reduction in fuel consumption when a SOFC-turbine power system using Jet-A fuel replaced the conventional gas turbine auxiliary power unit (APU) [11].

The conventional approach towards operating a SOFC with hydrocarbon fuels, such as Jet-A, requires an external fuel reformer to partially oxidize the fuel into CO and H_2 (i.e., "syngas"). Operating the SOFC by directly feeding the fuel into the cell − without the external fuel reformer − provides a very attractive way for utilizing the SOFC for providing electrical power because it significantly increases the breakeven weight: defined as the weight impact at which the additional fuel consumed as a result of the weight addition is equal to the fuel saved due to the higher efficiency of the generating system. So-called direct-liquid-fueled SOFCs internally reform the fuel followed by electrochemical oxidation reaction of the reformate within the anode [12].

Fuel cell technology is also of interest to hybrid electric automobile manufacturers and several companies, including Toyota and Honda, have released vehicles incorporating hydrogen-fueled fuel cell stacks [13,14]. Following the findings of the aircraft industry, replacing the internal combustion engine in an automobile with a fuel cell is most beneficial in terms of expected fuel savings when the fuel cell is fed directly with gasoline and the fuel cell becomes part of a hybrid system that includes batteries and other energy storage devices.

In order to fabricate an efficient gasoline-fueled SOFC, it is critical to develop an anode that can directly process the gasoline without coking and sulfur poisoning. While many possible anode materials have been studied including Ni, CeO_2, Cr- and Ti-based perovskites, and lanthanum vanadate [15–18], our group has focused on MoO_2 [19–21] .

Molybdenum dioxide is an unusual ceramic material in that it exhibits metallic-like electronic conductivity and this behavior is believed to lead to the high catalytic activity of MoO_2 towards partial oxidation of various hydrocarbons including isooctane, *n*-dodecane, and Jet-A fuel. Additionally, MoO_2 has been shown to have high resistance to coke formation due to its ability to selectively transport lattice oxygen to the surface of the catalyst, which lowers the possibility of carbon accumulation. Based on its high catalytic activity toward complex liquid fuels, its ability to conduct both electrons and ions, and its high coking resistance, a SOFC using a MoO_2-based anode was successfully fabricated and operated with a maximum power density output >3 W cm^{-2} being directly fed with *n*-dodecane (a jet fuel surrogate) [22].

The present letter reports the performance of a SOFC directly fed with premium gasoline. The results show the possibility of creating a direct gasoline-fed SOFC using a MoO_2-based anode that could be deployed in fuel-efficient hybrid electric vehicles that are quieter and less polluting than current gasoline and diesel powered engines. As noted earlier, a significant benefit of using fuels such as gasoline, rather than H_2, is that a robust distribution infrastructure is already in place.

2. Experimental

Electrolyte-supported fuel cells were fabricated using commercial single electrode cells (cathode side only) purchased from Fuel Cell Materials (Columbus, Ohio). The electrolyte was 8 mol.% yttria-stabilized zirconia (YSZ) with a thickness of 150 μm and a diameter of 12.5 mm. The cathode used in the commercial cells was A-site deficient $(La_{0.8}Sr_{0.2})_{0.95}MnO_3$ (LSM) with the geometrical surface area of 1.23 cm^2. Nanoparticle MoO_2 was synthesized as previously reported in the literature [22,23]. A suspension was prepared by mixing nanoparticle MoO_2 with ethylene glycol and nanopure water in a 1:1 volumetric ratio. After sonication, this

suspension was electrosprayed to form a seed layer on the anode side of the commercial cell. Electrospraying was performed for 2 h using the following operating parameters: substrate temperature at 300 °C; precursor suspension flow rate at 2 mL h^{-1}; and applied voltage at 10 kV. Subsequently, a thicker layer of catalyst was applied on top of the seed layer using a mixture of commercial MoO_2 (Alfa Aesar, Ward Hill, MA) and an aqueous solution of polyvinyl alcohol at 1:60 weight ratio. The geometrical area of the MoO_2-based anode was 0.785 cm^2. Silver paste was painted on the edge of both electrodes and attached to silver wires for current collection. A schematic of the MoO_2-based SOFC and the proposed operating concept is shown in Fig. 1. The liquid fuel used in this work was ethanol-free premium gasoline (Busch Distributors, Pullman, WA). The elemental composition of the gasoline was determined, using a Perkin Elmer 2400 Series CHN elemental analyzer, to be $C_{7.34}H_{11.93}$.

Cell performance and durability were measured using an experimental setup where the gasoline was first vaporized at 300 °C and carried to the cell by a mixture of air and CO_2. The molar composition of the fuel mixture used for the tests was: premium gasoline 18%, CO_2 45%, and air 37%. The CO_2 to air molar ratio and gasoline concentration in the fuel stream was determined on the basis of previous work carried out in our laboratory to stabilize the MoO_2 bulk phase by providing the optimum redox environment [24]. The operating cell temperature was fixed at 750 °C. The morphology of the anode was examined both pre-test and post-test using scanning electron microscopy (SEM; FEI Sirion operated at 15 kV). The bulk composition of the tested anodes was determined using a Phillips X-ray diffractometer with Co K_α radiation and an iron filter.

3. Results and discussion

The cell performance obtained over a representative 24 h period is shown in Fig. 2(a). As seen, the open cell voltage (OCV) at the beginning of the test was 0.91 V; it remains at this high initial value during the entire test. The current density was monitored at the cell voltage of 0.6 V. At the start of the run the current density was 5.4 A cm^{-2} and progressively decreased over the first 7 h to reach an average value of 3.1 A cm^{-2} for the remaining 17 h of the test. The corresponding drop in current density during the first 7 h may be the result of in-situ sintering of the MoO_2-anode layer and the concomitant decrease in surface area. The densification of the anode layer due to sintering would show a similar profile [25], but clearly further work is needed to better understand this aspect of cell performance.

Fig. 2(b) shows voltage and power density as a function of the current density after operating the cell for the first 1 h ($t = 1$ h),
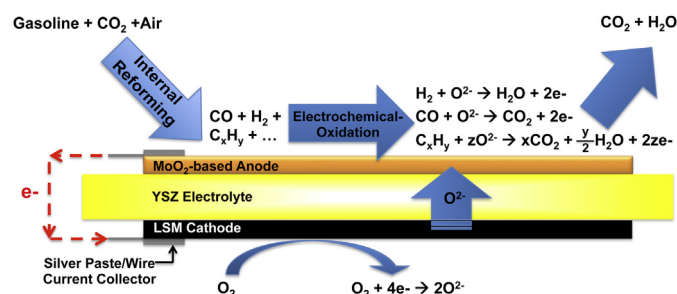

Fig. 1. Schematic of MoO_2-based SOFC operating with the premium gasoline fuel mixture.
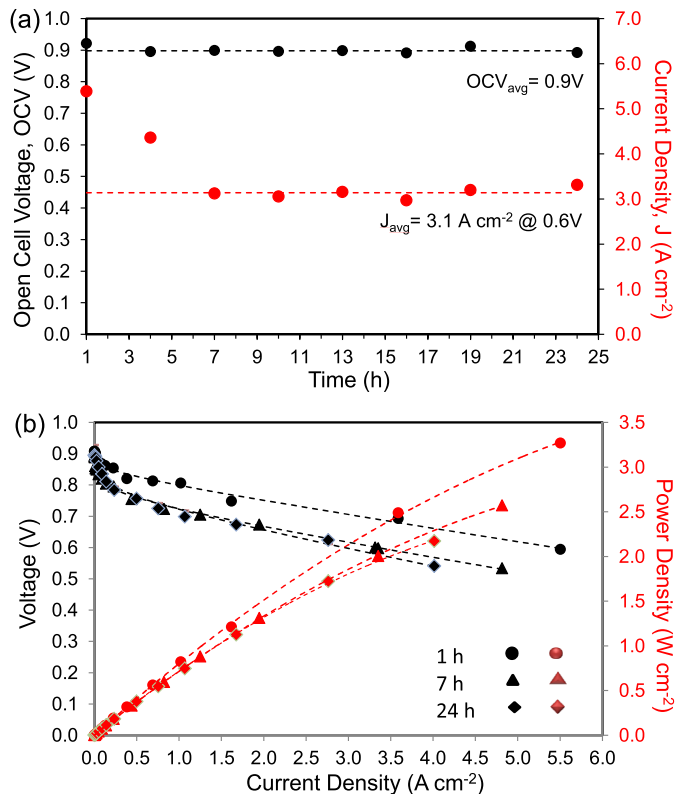
Fig. 2. (a) Plots of open cell voltage (OCV) and current density at 0.6 V as a function of operation time for the MoO₂-based SOFC. (b) Cell voltage and power density versus corresponding current densities of the MoO₂-based SOFC. The fuel mixture of premium gasoline, air and CO₂ is directly fed into the MoO-based anode, while ambient air was used for the cathode. The cell operating temperature was fixed at 750 °C.

after operating for the first 7 h ($t = 7$ h), and at the end of the test ($t = 24$ h). Initially ($t = 1$ h), the MoO₂-based SOFC produces the high power density output throughout the entire cell voltage range that we tested. For example, the cell initially generates the power density >3 W cm⁻² at 0.6 V. Its overall cell polarization resistance at the OCV condition estimated from the electrochemical impedance spectroscopy is ~7.2 Ω cm², which decreases down as the applied load increases (data not shown). Since the A-site deficient LSM cathode under the operating conditions used in the present study typically shows the polarization resistance value in an order of 0.1 Ω cm², we can assume that our measured overall cell polarization is mostly contributed by the MoO₂-based anode. Between the first 1 h and the first 7 h, the power density at 0.6 V decreases from 3.3 to 2.0 W cm⁻². However, it is very important to point out that the MoO₂-based SOFC show no further significant decreases in the cell performance for the remaining cell testing time. Thus, it still maintains a high power density output of 2.0 W cm⁻² at 0.6 V over 17 h following the initial drop.

From the voltage–current curves shown in Fig. 2(b), no mass transfer limited current densities were observed. Considering the absence of significant mass transport limitations, the cell voltage and current density can be related by the following simple expression [26]:

$$V = OCV - A \, Ln\left(\frac{j}{j_0}\right) - Rj \qquad (1)$$

where OCV represents the open cell voltage, A the Tafel slope, j the current density, j_0 the exchange current density, and R the cell resistance. For typical fuel cells, the cell voltage drops at near its OCV value (i.e., kinetic region of the current–voltage curve) is mostly contributed by its activation overpotential as described by the second term of the right-hand side of Eq. (1). On the other hand, the cell voltage drops over the linear region of its voltage–current curve is mostly contributed by its ohmic overpotential as described by the third term of the right-hand side of Eq. (1) [19]. According to
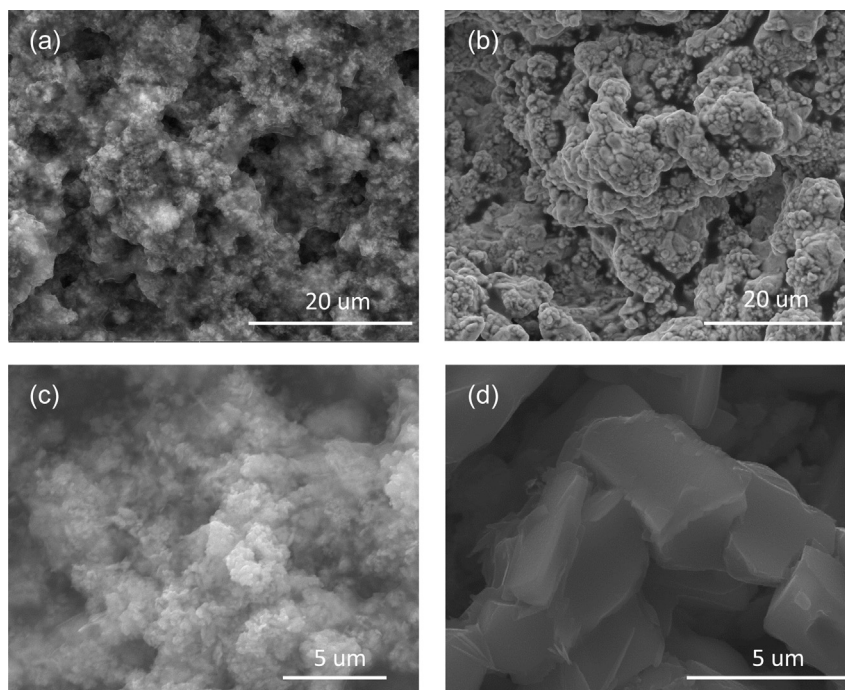

Fig. 3. SEM images of MoO₂-based anode showing surface morphologies. (a) and (c) Show fresh MoO₂-based anode, (b) and (d) show tested MoO₂-based anode after operating it for 24 h with gasoline. (d) Shows evidence of sintering and particle growth.

the voltage–current curves shown in Fig. 2(b), over the first 7 h of cell operation, the MoO_2-based SOFC shows much increased activation overpotential, while its ohmic overpotential does not significantly change as the slopes of its voltage–current curves are essentially same. It would require further investigations to exactly identify what factors contribute the most to the change of its activation overpotential value over the first 7 h of the cell operation.

X-ray diffraction (XRD) analysis (data not shown) was performed on the MoO_2-based anode before and after testing for 24 h to determine whether there were any bulk phase changes during cell operation. The data showed that the majority of the MoO_2 remained in the monoclinic polymorph with a small amount of an oxycarbide phase being formed. It has been previously reported that, under reforming conditions with lower O_2/C ratios, the MoO_2 phase can transform into carbide. The presence of an oxycarbide indicates that under the fuel cell environment the conditions favor the oxycarbide rather than the carbide.

Fig. 3 shows plan view SEM images of a MoO_2-based anode before and after testing for 24 h. After 24 h of operation, the morphology of the anode surface shows some evidence of sintering. The sintering can enhance the adhesion between MoO_2 particles, and hence it can improve the overall cell performance by decreasing the ohmic overpotential value [27]. However, over sintering can significantly reduce the available surface area for the electrochemical reactions. Because j_0 is an extensive parameter, its value decreases as the available electrode surface area is reduced [28]. Thus, over-sintering can increase the activation overpotential value of the MoO_2-based anode by decreasing its j_0 value according to the second term of Eq. (1). From the slopes of the ohmic region of the current–voltage plots shown in Fig. 2(b), the ohmic overpotential is very similar over the first 7 h of operation. Considering the fact that the activation overpotential increased significantly over the same cell operation time, it seems that the negative effect of the anode sintering (i.e., decrease of the active surface area) outweighs any positive effect (i.e., the decrease of cell resistance (R)). A notable absence from the SEM images of post-tested samples is evidence of coking. Thus, the MoO_2-based anode is able to resist coking under severe operating conditions when directly fed a gasoline mixture.

4. Conclusions

We have shown that SOFCs using a MoO_2-based anode can be successfully worked under direct gasoline-fed operating conditions with promising initial open cell voltage of ~0.9 V and high power density >3 W cm^{-2} at 750 °C. Under these harsh operating conditions, the MoO_2-based anode showed high resistant to coking and relatively stable cell performance over 24 h. Our results demonstrate that a MoO_2-based SOFC significant potential to efficiently generate electrical power for future hybrid electrical vehicles.

References

[1] S. Park, J.M. Vohn, R.J. Gorte, Nature Lond. 404 (2000) 265–267.
[2] Z. Shao, S.M. Haile, J. Ahn, P.D. Ronney, Z. Zhan, S.A. Barnett, Nature Lond. 435 (2005) 795–798.
[3] X.M. Ge, S.H. Chan, Q.L. Liu, Q. Sun, Adv. Energy. Mater. 2 (2012) 1156–1181.
[4] J. Ren, S.R. Gamble, A.J. Roscoe, J.T.S. Irvine, G. Burt, Fuel Cells 12 (2012) 773–786.
[5] T. Wei, Y.H. Huang, Q. Zhang, L.X. Yuan, Y.M. Sun, X.L. Hu, W.X. Zhang, J.B. Goodenough, Chem. Mater. 24 (2012) 1401–1403.
[6] M. Saidi, F. Siavashi, M.R. Rahimpour, J. Nat. Gas. Sci. Eng. 17 (2014) 13–25.
[7] S. Roychoudhury, M. Lyubovshy, D. Walsh, D. Chu, E. Kallio, J. Power Sources 160 (2006) 510–513.
[8] M.A. Azimova, S. McIntosh, J. Electrochem. Soc. 158 (2011) B1532–B1538.
[9] T. Tao, M. Koslwske, J. Bentley, J. Brodie, ECS Trans. 41 (12) (2012) 115–124.
[10] D. Daggett, in: "Fuel Cells & Hydrogen Airplanes", Presented to Canada and US Fuel Cell & Hydrogen Partner Meeting, Seattle, WA, 2004.
[11] D. Daggett, N. Lowery, J. Wittmann, in: "Fuel Cell APU for Commercial Aircraft", Presented at The H2Expo, Hamburg, Germany, Sept. 2005.
[12] O. Marin-Flores, T. Turba, C. Ellefson, K. Wang, J. Breit, J. Ahn, M.G. Norton, S. Ha, Appl. Catal. B Environ. 98 (2010) 186–192.
[13] Toyota Motor, The Toyota Fuel Cell Vehicle, 2014. Available, http://www.toyota.com/fuelcell/.
[14] Honda Motor Co, Fuel Cell Electric Vehicle, 2014. Available, http://automobiles.honda.com/fcx-clarity/.
[15] A. Atkinson, S. Barnett, R.J. Gorte, J.T.S. Irvine, A.J. McEvoy, M. Mogensen, S.C. Singhal, J. Vohs, Nat. Mater. 3 (2004) 17–27.
[16] E.P. Murray, T. Tsai, S.A. Barnett, Nature Lond. 400 (1999) 649–651.
[17] H. Yokokawa, N. Sakai, T. Kawada, M. Dokiya, Solid State Ionics 52 (1992) 43–56.
[18] S. Tao, J.T.S. Irvine, J. Solid State Chem. 165 (2002) 12–18.
[19] O. Marin-Flores, S. Ha, Appl. Catal. A Gen. 352 (2009) 124–132.
[20] B.W. Kwon, C. Ellefson, J. Breit, J. Kim, M.G. Norton, S. Ha, J. Power Sources 243 (2013) 203–210.
[21] O. Marin-Flores, L. Scudiero, S. Ha, Surf. Sci. 603 (2009) 2327–2332.
[22] B.W. Kwon, S. Hu, O. Marin-Flores, M.G. Norton, J. Kim, L. Scudiero, J. Breit, S. Ha, Energy Technol. 2 (5) (2014) 425–430, http://dx.doi.org/10.1002/ente.201300165.
[23] C.A. Ellefson, O. Marin-Flores, S. Ha, M.G. Norton, J. Mater. Sci. 47 (2012) 2057–2071.
[24] O. Marin-Flores, T. Turba, J.B. Ellefson, M.G. Norton, S. Ha, Appl. Catal. A Gen. 381 (2010) 18–25.
[25] C.B. Carter, M.G. Norton, Ceramic Materials: Science and Engineering, second ed., Springer, New York, 2013, p. 444.
[26] S.H. Chan, K.A. Khor, Z.T. Xia, J. Power Sources 93 (2001) 130–140.
[27] J. Hong, S. Ida, T. Ishihara, Solid State Ionics 262 (2014) 374–377.
[28] H.S. Song, W.H. Kim, S.H. Hyun, J. Moon, J. Kim, H.W. Lee, J. Power Sources 167 (2007) 258–264.